IJCRT.ORG ISSN : 2320-2882

INTERNATIONAL JOURNAL OF CREATIVE RESEARCH THOUGHTS (IJCRT)

An International Open Access, Peer-reviewed, Refereed Journal

Moving Toward A Wearable System To Anticipate A Freeze Of Gait In Parkinson's Disease Patients

[1]Mrs.S.SasiRekha, [2]Dr.R.Shankar, [3]Dr.S.Duraisamy

[1]Research Scholar, [2]Associate Professor, [3]Assisstant Professor
[1]Department of Computer Science,
[1]Chikkanna Government Arts College ,Tirupur, India

***Abstract*—** A few wearable technologies that take advantage of on-body acceleration sensors have been put forth to identify Freezing of Gait (FoG) in Parkinson Disease (PD) patients. These devices produce a series of rhythmic stimuli in response to the detection of a FoG event, enabling the patient to resume the march. Although these methods work well at identifying FoG occurrences, they cannot foresee FoG in order to stop it from happening. To bridge the gap, a machine learning-based method for classifying accelerometer data from Parkinson's disease patients is presented in this study. It can identify a pre-FOG phase, which helps to further predict the onset of FoG ahead of time.

Three tri-axial accelerometer sensors—one each on the back, hip, and ankle—were used to track the subject's gait. The raw accelerometer data was then windowed and non-linear dimensionality reduced to extract gait features. Three groups of events (pre-FoG, no-FoG, and FoG) were utilized to categorize gait using the k-nearest neighbor method (k-NN). The suggested solution's accuracy was evaluated against cutting-edge methods. Our research demonstrated that: (i) we were able to detect FoG with performances that were better than those of the state-of-the-art methods; (ii) we were able to predict FoG by identifying the pre-FoG events with an average sensitivity and specificity of, respectively, 94.1% and 97.1%; and (iii) our algorithm could be used on devices with limited resources for the first time in the literature. upcoming uses comprise *Index Terms*—freezing of gait, wearable device, accelerometer, explainable machine learning, classification.

I. INTRODUCTION

Parkinson's disease (PD) is the second most common neurodegenerative disorder. Falls are the most disabling complications of advanced PD leading to increased risk of hospitalization, immobilization, comorbidity and disability, [1]. Among PD patients, 35-90% fall once a year, and 18-65% fall repeatedly (range:4.7-67.7 falls/person/year) [2]. At least 20% of falls can be attributed to a single PD symptom, known as freezing of gait (FoG), which affects around 50% of patients [3]. FoG is an episodic gait disturbance lasting up to 30'' with different phenomenology that ranges from complete sudden akinesia to milder leg trembling or short shuffling steps events, usually described by patients as feeling the feet stuck to the floor [4]. FoG is a poorly recognized symptom, because of its episodic nature, the bias in the interpretation and report of this symptom by patients, and the need of an observer [5]. Different treatment strategies have been proposed for FoG, but the results are controversial, and evidence of efficacy still limited [6]. A minority of patients with FoG respond to levodopa, monoamine oxidase inhibitors, deep brain stimulation and levodopa-carbidopa intestinal gel, but often FoG is caused/worsened by treatment or drug-resistant [7].

The high incidence of FoG and the difficulties in its assessment and treatment by standard clinical methods have led to investigate wearable devices and machine learning algorithms [8]. Most of them deal with recognizing FoGevents by building on top of offline datasets gathered from thepatients through wearable devices equipped with different sensors, e.g., accelerometers [9,10], gyroscopes [11], EEG sensors [12,13], EMG [13,14], and force and bending sensors[15]. These solutions are primarily devoted to study FoG features. In some cases, the devices provide patients with rhythmic visual, sensory or auditory stimuli upon FoG detection [8,16] to reduce its duration. This approach builds on the observation that PD patients more easily exit FoG whenthey are externally stimulated with a Rhythmic Auditory Stimulation (RAS), which focuses the attention during movement [17].

Different statistical methods have been investigated to increase accuracy of FoG recognition. They include the use statistical features over raw sensor signals [18], and the freezing index, i.e., the ratio between FoG and no-FoG frequency bands [9]. Approaches based on Inertial Measurement Unit (IMU) incorporating accelerometer, magnetometer and gyroscope sensors [10,11], and using different recognition algorithms (i.e. Random Forest, C4.5, Naive Bayes, k-NN, Logistic Regression and Support Vector Machine (SVM) [18,19,20] or Deep Learning approaches [11, 21]. High levels of accuracy, and short lag times in FoG and pre-FoG detection are key features in this field. A recent comprehensive review on performances of wearable sensors to detect FoG detection reported 73–100% sensitivity and 67–100% specificity [22].

While several studies focused on FoG detection, only a small number of them assessed pre-FoG recognition. A methodology to detect FoG, pre-FoG and no-FoG was proposed with 94% accuracy [23]. Furthermore, t-Distributed Stochastic Neighbour Embedding (t-SNE) was proposed as feature projection algorithm and tested on different machine learning models obtaining balanced accuracies of 91%, 90% and 82% for FoG, pre-FoG and no-FoG detection,

respectively [24]. Other studies based on datasets gathered through inertial sensors on the feet and back achieved average precision of 83% and recall of 67% [10], while a deep learning approach based on the data collected by a single IMU device located on the patient's waist achieved 90% of geometric mean between precision and recall [11]. Other approaches to detect pre-FoG [25, 26] were based on the recognition of EEG pattern [27], the analysis of data gathered by wearable sensors [10], electrocardiography and skin-conductance [12,18]. Two novel algorithms for FoG prediction, based on the DAPHNET dataset and tested on neural network model [23] and a pool of machine learning models [24] were also proposed.

In summary, only few techniques have been proposed for predicting pre-FoG patterns in gathered data, and more research is necessary on this topic. In addition, almost all the methods mentioned above run on a server instance, because of the complexity of the pattern recognition and feature extraction algorithms, which require high computational resources to achieve high sensitivity and specificity, hampering their use on small wearable devices. Because of these limitations, we present a new approach, based on wearable devices and machine learning algorithms to detect FoG, pre-FoG and no-FoG in PD patients and that can be for a wearable system. The future application will be to develop an on-demand cueing device to help PD patients to overcome FoG and prevent falls.

The rest of the paper is organized as follows. Section II introduces preliminary concepts. Section III details the study protocol and presents the technical details of the proposed methodology. Section IV describes the experimental results, including the characteristics of study population. Results are then further discussed in Section V. Finally, Section VI draws the conclusions with the proposal of future work.

II. Preliminaries on Machine Learning

A. Feature extraction

In most classification pipelines, raw data are typically pre-processed to project them into different feature spaces where classification is made easier (typically, linear). This pre-processing stage is known as feature extraction [28]. The most used algorithms for feature extraction are summarized in the next paragraphs.

1) Principal Component Analysis (PCA) is the most common technique for reducing the dimensionality of a large set of possibly correlated features [28]. It consists of a roto-translation of the original vector feature space, obtaining anew set of bases aligned with the most data variation. The reduction consists in projecting the data on a subset of these bases, retaining less features than the original ones.

2) kernel PCA (kPCA) uses the theory of the positive definite kernel and reproducing kernel Hilbert space [28] for doing (implicitly) PCA on data projected in an infinite-dimensional space. The result in the original feature space is a non-linear projection way more effective that the original PCA, with the additional cost of choosing a proper kernel and its parameterization.

3) Linear Discriminant Analysis (LDA) is a generalization of the Fisher's linear discriminant, a method to find a linear combination of features that separates samples of different classes. LDA is more effective than PCA when it comes to multi-class problem, but it requires to know in advance the label of each training data [29].

4) kernel LDA (kLDA) is a kernel-based version of LDA. Using the kernel substitution, LDA is performed in a new feature space, which allows non-linear mappings to be learned [30].

B. Classification

To determine which class in a pool of classes best explains a new observation, standard classification quantities are used. It is the most popular machine learning process, and feature extraction is crucial to its success. Typically, it begins with a training phase in which a classification algorithm uses a training set of D-dimensional data to develop a classifier. Each training sample in supervised classification has a class-label characteristic that indicates the class to which it belongs. Next, a test D-dimensional input sample that has not yet been viewed is utilized to predict the class label using the trained classifier.. The most common classification quality metrics are [31]:

$$Precision = P \quad P_{true\ positive} \quad P$$

$$Recall = P \quad P \quad false\ negative$$

$$Specificity = \frac{P \quad true\ P}{false\ positive + \quad true\ negative}$$

$$F1 — \quad precisiotnrurecnaellgative \quad true\ positive + false\ positive \quad precision + recall$$

where *precision* and *recall* (also known as *sensitivity*) measure how much the classifier is capable of avoiding false positives, and is capable to correctly classify all of the samples of aclass, respectively, while *specificity* and *F1-Score* measure the classifier ability to correctly classify true negatives and the harmonic average of precision and recall, respectively.

III. Study Protocol

The proposed approach addresses the application scenario showed in Figure 1. The patient's gait is monitored by three tri-axial accelerometer sensors worn on his/her back, hip and ankle. Features are then extracted from the accelerometer's raw data through data windowing and non-linear dimensionality reduction. A *k*-nearest neighbor algorithm (*k*-NN) [28] is finally used to classify patient's gait in three classes of events: pre-FoG, no-FoG and FoG. To address this scenario, we developed a workflow composed of two main phases: *1) offline training data pre-processing* and *2) on*

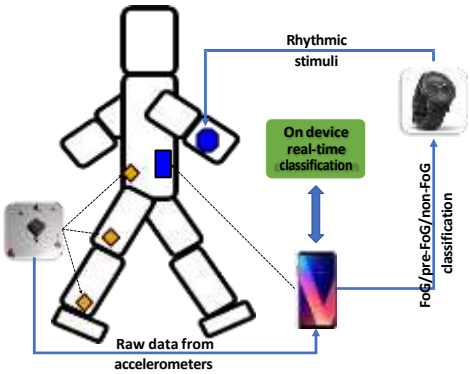

Figure 1. Application scenario

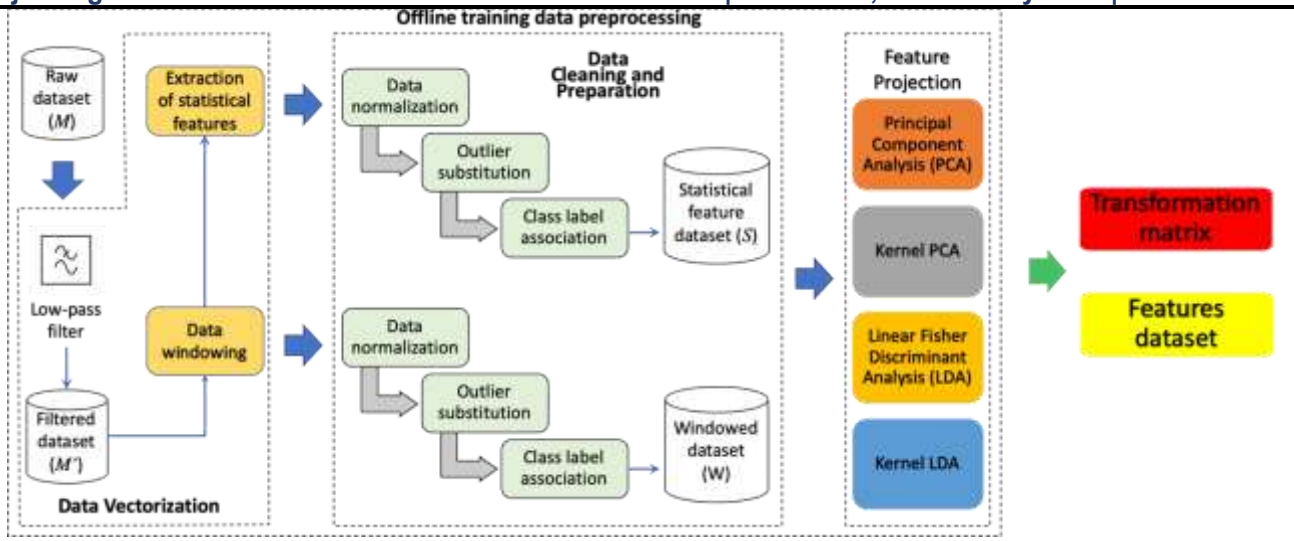

Figure 2. Detailed workflow of the offline pre-processing phase.

device real-time classification, described in detail below.

A. Offline training data pre-processing

The input data is constituted by raw values gathered during patient's gait from three accelerometers. In particular, the atomic entity of the input is the record, i.e., a vector composed of 9 elements (3 per each accelerometer) measuring the acceleration of the patient in a specific instant with respect to the three axes of a Euclidean space. The number n of records in a given interval depends on the accelerometer sampling rate. Thus, the input dataset is as a matrix M with n rows and 9 columns. The final goal is to set up a classification method exploiting the k-NN algorithm on time windows, capable of

forecasting when a FoG event is going to happen, i.e.,

detecting what we call a pre-FoG event.

The raw data included in the training matrix M are pre-processed to generate two alternative datasets: a windowed dataset W, and a statistical feature dataset S. The pre-processing phase performs a *data vectorization* step, followed by *data cleaning and preparation*, and finalized by a *feature projection* procedure. The detailed workflow is shown in Fig. 2 and detailed hereafter.

1) Data vectorization: A low-pass filter is firstly applied to the elements of M to obtain a new matrix M', where the sensor noise is reduced. Then, two alternative steps are performed starting from M': *data windowing* and *extraction of statistical features*.

In *data windowing*, the rows of M' are grouped according to time windows of size w seconds with an overlap of t seconds. For example, in case the sampling frequency is 1Hz[1] with w = 3 and t = 1, the data included in rows 1-3 of M' are associated to the first-time window and they become, preserving their order, the elements of the first row of matrix W. Then, the data included in rows from $w-t$ = 2 to $w-t+w$ = 5 of M' become the elements of the second row of W, and so on. The size of W is then $m \times 9 * w$, where m is the total number of time windows.

During the *extraction of statistical features*, a new matrix S is generated from W by extracting 129 statistical features per each row of W. Thus, the size of S is $m \times 129$. The extracted features are similar to those used in a previous study [12], e.g., variance, mode, standard deviation, maximum and minimum values of raw data.

2) Data cleaning and preparation: Subsequently, the normalization of the values in W and S takes place. A unity-based normalization [32] is carried out over the elements of both W and S. The goal is to re-scale the values of W and M into the range [0, 1] by using equation 1, where X is a generic element of the matrix, while X_{min} and X_{max} are the minimum and the maximum value in the matrix:

$$X^0 = \frac{X - X_{min}}{X_{max} - X_{min}} \quad (1)$$

At this time, the next transformation step, for both matrices, is the outlier substitution. An outlier is a value that is more than 3 median absolute deviation away from the median [33]. Each outlier in W and S is substituted with the corresponding nearest not-outlier value.

At the final step of the pre-processing phase, each row of both matrices W and S is associated to a class label that represents the movement pattern observed on the patient during the corresponding time window. Such labels can be no-FoG, FoG and pre-FoG. Consistently with the existing literature [10,12], we assume the gait performance of PD patients deteriorates in the phase immediately preceding a FoG event. The association is assigned such that FoG is used when the time window includes at least one sample where the patient actually experiences a FoG episode; pre-FoG is assigned to the time windows of type no-FoG immediately preceding a FoG time window by at maximum s seconds, where reasonable values for s are between 2 and 4 seconds; finally, no-FOG is used for all the remaining time windows.

3) Feature projection: In the final step, we use four different feature projection algorithms to explore which of them performs better in our scenario. The experimental analysis is

[1] 1Hz is a too low frequency for predicting FoG. It has been assumed for simplifying the exemplification. The dataset used in our experiments has been created at 65Hz.

performed in four different ways according to the applied training features and the number of target classes considered for the classification. The four alternatives are: (i) training features extracted from *W*, and 2 classes (FoG, no-FoG); (ii) training features extracted from *W*, and 3 classes (FoG, no-FoG, pre-FoG); (iii) training features extracted from *S*, and 2 classes (FoG, no-FoG); (iv) training features extracted from *S*, and 3 classes (FoG, no-FoG, pre-FoG).

For each of the previous alternatives, PCA, kPCA, LDA and kLDA are applied for extracting the final projected features to be provided to the *k*-NN classifier. In Section IV, we will show that alternatives 1 and 2 associated with the kLDA algorithm provide the better results. Finally, as shown in Fig. 3, the training data pre-processing phase returns the new training features dataset and the transformation matrix that are the input for the on device real-time classification phase.

B. *On device real-time classification*

Our system is intended to be used for real-time classification of FoG, no-FoG and pre-FoG directly on the patient. Thus, after the off-line training data preprocessing, the workflow proceeds as shown in Fig. 3. The data gathered by the accelerometers on the patient body are transmitted to the mobile phone through the Bluetooth Low Energy (BLE) protocol. Once the data are received, they are elaborated through the same data vectorization process presented in Section III.A.1. After vectorization, the data are multiplied with the transformation matrix obtained by the offline data preprocessing phase, projecting into a reduced features space (p_1, ..., p_f), where, f (≥ 1), defines the number of features generated after the projection. In the case of the LDA and kLDA algorithms f will be equal to the number of treated classes (no-FoG, FoG, and pre-FoG) minus one. Finally, such new features are passed to the *k*-NN classifier that, based on the training feature dataset, recognizes the movement as FoG, no-FoG or pre-FoG. It is worth noting that the use of the *k*-NN ensures fast performances and no need of an explicit training procedure. In fact, we have solely training features that are used as comparison w.r.t. the testing data.

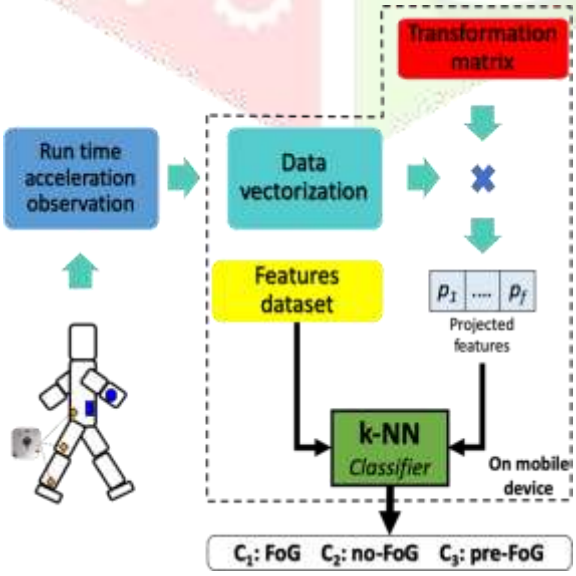

Figure 3. On device real-time classification.

IV. RESULTS

A. *Patient population*

In order to achieve findings that are both expressive and comparable to those found in relevant literature, we implemented the suggested method using the DAPHNET benchmark suite, a commonly used gait dataset that was gathered in 2010 as part of the EU FP6 project Daphnet [9]. Video and gait data of PD patients who had a history of FoG and were able to walk alone during OFF phases were recorded as part of the study's original methodology. Severe visual or hearing loss, dementia, or indications of other neurological or orthopedic conditions were considered exclusion criteria. A total of ten patients (7 males, mean age 66.5±4.8, mean disease duration 13.7±9.7, mean Hoehn & Yahr score in ON 2.6±0.65) were enrolled and participated in the entire study. Eight had several FoG events (average of 23.7 FoG events per patient), while two did notThe first part of the study s dedicated to application of the proposed methodology to the DAPHNET dataset, the second to on-line testing of the classification performance on different mobile devices, to evaluate its suitability on devices with lowcomputational resources.

B. *Dataset pre-processing*

Following the procedure described in Section III.A, starting from the DAPHNET data, we generated two different datasets, the windowed dataset *W* and the statistical feature dataset *S*. Both *W* and *S* depend on the time window size *w* and the overlapping parameter *t* to collect short overlapping sequences of acceleration values. Thus, we performed grid search on *w* and *t*; specifically, we varied *w* in the range [1:6] with step 1, and for each *t*, *t* assumed values in the range [0:*w*/2] with step 0.5, ending up with 27 (*w* ,*t*) combinations. For every combination (w_i, t_i), $1 \leq i \leq 27$, a couple (W_i, S_i) of different datasets was created. Then, we performed the feature-wise data normalization and the outlier removal. Finally, for each (W_i, S_i), we re-label as pre-FoG all windows immediately preceding a FoG window, obtaining a novel class, namely the pre-FoG. The introduction of pre- FoG windows shrank the distribution of no-FoG windows, on average, of a factor 1/8.

C. *Results for the windowed dataset*

Experimental results are reported in Table I, Table II and Table III. The classification of our approach has been cross-validated by extracting from DAPHNET training and testing partitions using *k*-fold (k = 3, 5) and leave-one-out schemes on individual patient and also cross-patient. It is worth noting that training and testing partitions were curated so that no partial overlap between windows was present. No significant difference was observed with these cross-validation schemes. Thus, for lack of space, in the following, we report and comment only the results achieved by using *k*-fold with k = 3.

Patient ID	#no-FoG	#FoG	PCA	kPCA	LDA	kLDA	#no-FoG	#pre-FoG	#FoG	PCA	kPCA	LDA	kLDA
P_01	465	18	0.72	0.70	0.64	0.99	460	5	18	0.44	0.43	0.42	0.86
P_02	124	9	0.64	0.63	0.61	0.99	120	4	9	0.31	0.32	0.31	0.96
P_03	405	68	0.75	0.73	0.73	0.99	357	48	68	0.39	0.42	0.40	0.84
P_05	263	120	0.72	0.70	0.70	0.99	243	20	120	0.17	0.18	0.18	0.96
P_06	526	33	0.68	0.66	0.65	0.98	514	12	33	0.44	0.44	0.46	0.98
P_07	362	12	0.57	0.56	0.55	0.99	356	6	24	0.38	0.36	0.39	0.99
P_08	203	53	0.78	0.77	0.73	0.99	194	9	53	0.48	0.41	0.42	0.94
P_09	471	128	0.85	0.84	0.82	0.99	463	8	128	0.58	0.61	0.60	0.98
	2-Class						3-Class						

Table I. Average F1-Score, at varying of w and t, respectively, in [1, 6] with step 1 and [0, w/2] with step 0.5.

Name	2-Class Sensitivity	2-Class Specificity	2-Class F1	3-Class Sensitivity	3-Class Specificity	3-Class F1
PCA	0.72	0.71	0.71	0.40	0.49	0.44
kPCA	0.71	0.69	0.70	0.40	0.48	0.44
LDA	0.68	0.67	0.68	0.40	0.48	0.44
kLDA	0.99	0.99	0.99	0.94	0.97	0.94

Table II. Average sensitivity, specificity and F1-Score, at varying of w and t, respectively, in [1, 6] with step 1 and [0, w/2] with step 0.5.

	Existing approaches [6]	[18]	[4]	Our approach kLDA
Sensitivity	0.92	0.98	0.87	0.99
Specificity	0.89	0.99	0.92	0.99
F1-Score	0.90	0.98	0.90	0.99
Method	Fourier	AdaBoost	SVM	*k*-NN

Table III. Comparative sensitivity, specificity and F1-Score of the proposed approach with respect to state-of-the art approaches on 2-Class classification.

Tables I, II and III refer only to the experiments conducted by using the windowed dataset *W*, because, as shown later in Section IV.D, this configuration guarantees the best performances with respect to using the statistical feature dataset *S*. The tables report the average results obtained by varying *w* and *t*, respectively, in the ranges [1, 6] with step 1 and [0, *w*/2] with step 0.5. Concerning the feature extraction algorithms, for kPCA and kLDA we tested the Gaussian, the polynomial and the linear kernel. The best result was obtained with the Gaussian kernel that the results in Tables I, II, III refer to. The Gaussian kernel parameters have been found by cross validation. Specifically, for each patient with FoG episodes, Table I shows the average F1-Score, for both 2-Class (no-FoG, FoG) and 3-Class (no-FoG, FoG, pre-FoG) cases, achieved by applying different strategies for feature projection. Columns #no-FoG and #FoG indicate the number of windows that have been labelled as normal and freeze of gait, respectively. Column #pre-FoG instead refers to the number of windows preceding those labelled with FoG. It turns out that, by construction, #pre-FoG indicates how many FoG episodes are in the data of each patient. As shown, kLDA achieves very good results for both 2-Class and 3-Class problems.

Table II shows the average Sensitivity, Specificity and F1-Score among all the 8 patients of Table I. The worst case is given by the PCA, while the best results are achieved with kLDA. This clearly implies that the classes cannot be linearly separated, highlighting the considered problem is challenging. Supervised feature extraction approaches (LDA, kLDA) work better than the unsupervised counterparts (PCA, kPCA) especially in the 3-Class case. In the 2-Class case LDA is almost equivalent to PCA probably due to the low dimensionality of the former (= 1).

To analyze more deeply the achieved results, Fig. 4 reports two confusion matrices related to patient 3, which, according

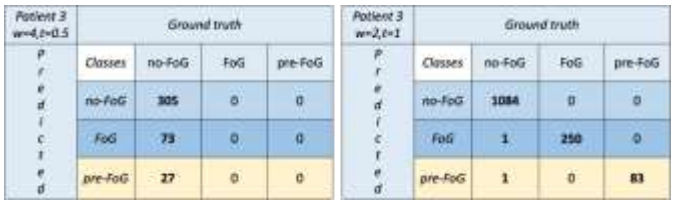

Figure 4. Worst case (left) and best case (right) confusion matrices for Patient 3 at varying (w, t).

to Table I, exhibits the lowest average F1-Score (84% with kLDA). By analyzing the results achieved for each configuration of parameters *w* and *t*, we discovered that the configuration (*w*=4, *t*=0.5) provides the worst results, as the classifiers erroneously recognizes the instances of FoG and pre-FoG as no-FoG (Fig. 4 left panel). On the contrary, the best results are achieved by using the configuration (*w*=2, *t*=1), where the classifier has almost always recognized the correct class (Fig. 4, right panel). Similar confusion matrices were obtained for the other patients. Selecting the correct (*w*, *t*) configuration is then fundamental for an effective classification. In almost all cases, the configuration (*w*=2, *t*=1) guarantees the best Sensitivity and Specificity.

Table III compares our approach, on the DAPHNET dataset, with three state-of-the-art techniques [9,18,19]. Only a comparison with the 2-Class problem was possible, as the considered works do not use the pre-FoG label, since they are focused on FoG detection rather than FoG prevention.

D. Results for the statistical feature dataset

Previous tables refer to results on the windowed dataset *W*, as the statistical feature dataset *S* gave worse performance. To better clarify the different results achieved by *W* and *S*, Fig. 5(a) and 5(b) present the mapping after applying Gaussian kLDA on, respectively, *W* and *S*, for patient P1, with *w*=4 and *t*=1, for the 3-Class problem. kLDA clearly separates samples of different classes, i.e., no-Fog (blue), FoG (red) and pre-FoG (yellow) on the *W* dataset (Fig. 5(a)), while this is not true for the *S* dataset (Fig. 5(b)). Similar results, omitted for lack of space, were obtained for the other patients.

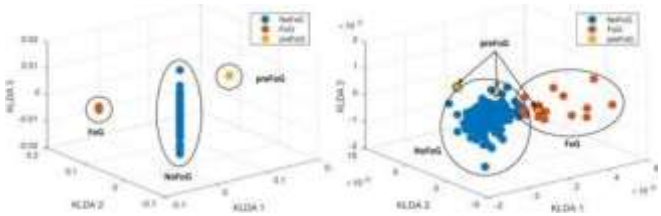

Figure 5. Results of the kernel linear discriminant analysis on Patient P1 with w=4 and t=1 using the (a) windowed dataset and (b) statistical feature dataset. Classes are clearly separated in (a), the same is not true in (b).

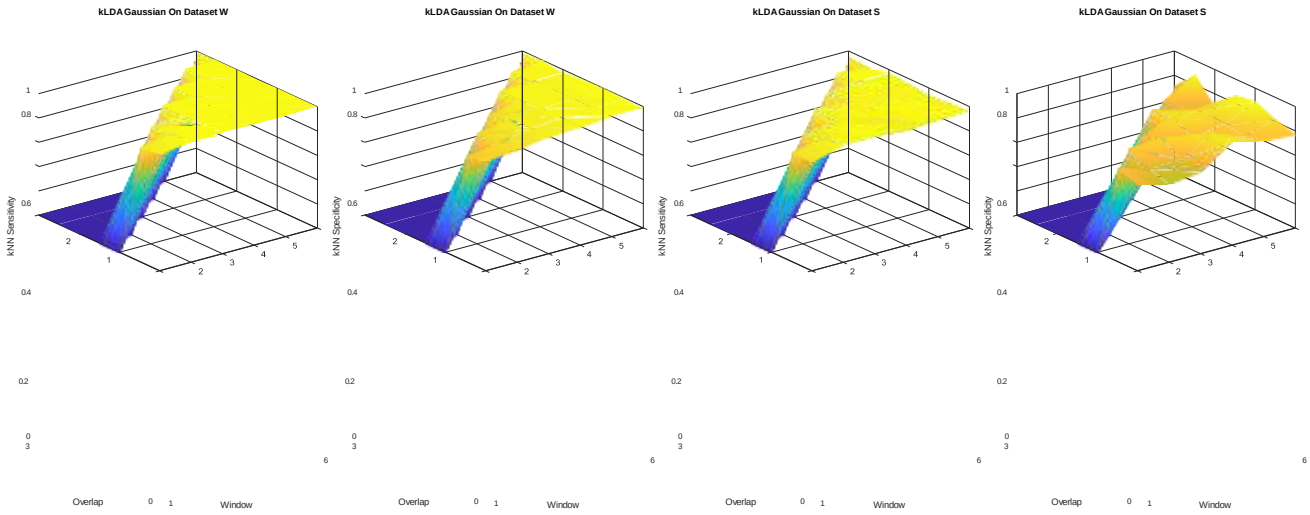

(a) (b) (c) (d)

Figure 6. Average sensitivity (a) and specificity (b) using W, and average sensitivity (c) and specificity (d) using S, obtained with kLDA at varying of the window size w and the overlap interval t.

Fig. 6 further highlights how the *W* dataset outperforms the*S* dataset for the 3-Class problem. Fig. 6(a) and 6(b) show, respectively, the average Sensitivity and Specificity on *W* for all the possible configurations of (*w, t*) and for all patients (P1, ..., P10). Fig. 6(c) and 6(d), instead, show average Sensitivity and Specificity on *S*. In Fig. 6(a) and 6(b) Sensitivity and Specificity achieved approximately 98%, while in Fig. 6(c) and 6(d) they reached approximately 94% and 70%.

E. Performance on mobile device

We evaluated the classification performance on three different smartphones in terms of response latency, RAM and ROM memory and battery consumption. Table IV shows the features of the tested smartphones (upper part) and the outcomes (lower part). *Latency* was the time spent for the computation of the workflow presented in Fig. 2, i.e., the time elapsed from the reception of the input data gathered from the accelerometers till the classification of patient's gait. The time taken to transmit data from the accelerometers to the smartphone and the stimulus command from the smartphone to the smartwatch is negligible. ROM and RAM memories were mainly used to save the transformation matrix and the features dataset obtained after the offline training data pre-processing phase (Fig. 3). Battery consumption shows the average consumed battery for a total of 10 hours. Regarding the quality of classification, the results were equal to those obtained in computation on an external server machine (Tables I, II and III).

Metrics	Nexus5	S7 Edge	6T
CPU (GHz)	2.3	2.3	2.8
Core	Quad	Octa	Octa
RAM (GB)	2	4	6
ROM (GB)	16	64	128
Battery Capacity (mAh)	2300	3600	3700
Latency (ms)	≈ 120	≈ 100	≈ 105
Used ROM (Mb)	≈2	≈2	≈ 2
Used RAM (Mb/h)	113	114	120
Battery Consumption (mAh)	78	76	80

Table IV. Device performance metrics.

V. DISCUSSION

We presented a methodology based on machine-learningalgorithms to classify the PD gait features as pre-FoG, FoG,and no-FoG patterns with a wearable system. Our results provethe effectiveness of the proposed FoG prediction and show thepossibility of implementing our solution on a wearable system.We compared the present approach with three state-of-the- art ones, in terms of Sensitivity, Specificity and F1-Score: the2-Class and 3-Class classification (Table III) outline the better performance of the proposed algorithm, compared to previous2-Class [9,18,19], and 3-Class ones [23,24], with a higher, onaverage over 2%, overall accuracy. In particular, our solution with kLDA achieved the best results. It is worth noting that the*k*-NN is a less complex classification algorithm than those based, respectively, on AdaBoost, SVM, and fast Fouriertransform [9,18,19], and is more suited for a real-time classification on a wearable device with limited computing andmemory resources. Moreover, our approach achieved very good results on different configurations of window size *w* and overlap interval *t*, in particular when the windowed dataset *W* is used (Fig. 6). Finally, 3-Class classification permitted the prediction of FoG *w* seconds in advance.

One of the main limitations of the existing approaches for FoG detection is that the classification phase requires to offload the computation to an external server, due to high computing resources. On the contrary, we proved our classification algorithm can be executed on a resource- constrained device, like a smartphone. Classification performance, response latency, RAM and ROM memories andbattery consumption did not differ significantly among the three mobile devices tested. These finding confirm the overall"lightness" of the algorithm, thanks to the used classifier and the reduction in the number of processed features, with no detrimental effect on the overall classification accuracy. This point is of outmost importance since, differently from alreadyexisting solutions, it removes the need to reach an external server, that may result in unpredictable delays. In addition, thesystem can work even in absence of an Internet connection.

Our study has some limitations. The sample size of DAPHNET project was small. Moreover, FoG has different subtypes and may be caused by different triggers in PD [5,34]. FoG events in the DAPHNET dataset [9] were not classified according to subtypes, so we could not test if our detection algorithm can classify pre-FoG, FoG and no-FoG, with a similarly high performance for all FoG subtypes. Further studies with larger patients' samples and different FoG subtypes are necessary to confirm the reproducibility of our results. Further, we applied the algorithm off-line to a pre-existing dataset, so confirmatory studies are necessary to evaluate its on-line performances. Finally, computational sustainability was tested on smartphones. Our algorithm should be tested on devices with even less computationalresources (e.g., smartwatches), to support its use on wearable on-demand cueing device.

VI. CONCLUSION AND FUTURE WORK

PD patients can overcome the impairment of FoG using external cueing, a non-pharmacologic treatment.one of the pathophysiological mechanisms of FoG, involuntary movement, by altering gait to a goal-directed movement that is less compromised by Parkinson's disease [35]. Various devices have been presented that couple a detecting system with the transmission of a cueing stimulus. Only three of these devices, out of the five that have been evaluated on PD patients to the best of our knowledge, have been found to be beneficial in lowering the frequency and duration of FoG [16]. Nevertheless, the quality of the studies was generally low (quasi-experimental, low statistical power), and the various methodologies made it difficult to conduct a meta-analysis or a direct comparison.

The high accuracy and short lag times between pre-FoG recognition and cueing administration are critical to a cueing on-demand wearable device's overall effectiveness in reducing FoG and falls in Parkinson's disease. Subsequent research endeavors ought to delve into the online efficacy and precision in delivering the cue of our high-performance classification system among people with Parkinson's disease.

.

REFERENCES

[1] L.V. Kalla, A.E. Lang. Parkinson's disease, Lancet, vol. 386, no. 9996, pp. 896-912, 2015.

[2] N.E. Allen, A.K. Schwarzel, C.G. Canning. Recurrent Falls in Parkinson's Disease: A Systematic Review. Parkinson's Disease, no. 906274, 2013.

[3] M. Rudzinska, S. Bukowczan, J. Stozek, K. Zajdel, E. Mirek, W.N. ChwaÑa, M. Wójcik-Pêdziwiatr, K. Banaszkiewicz, A. Szczudlik. Causes and Consequences of Falls in Parkinson Disease Patients in a Prospective Study, Neurologia i Neurochirurgia Polska, vol. 47, no. 5,

pp. 423-430, 2013.
[4] M.D. Latt, S.R. Lord, J.G. Morris, V.S. Fung. Clinical and physiological assessments for elucidating falls risk in Parkinson's disease. Movement Disorders vol. 24 no. 9 pp. 1280–1289, 2009.
[5] B. R. Bloem, J. M. Hausdorff, J. E. Visser, N. Giladi. Falls and Freezing of Gait in Parkinson's Disease: A Review of Two Interconnected, Episodic Phenomena. Movement Disorders, vol. 19, no. 8, pp. 871-884, 2004.
[6] J. Nonnekes, A.H. Snijders, J.G. Nutt, G. Deuschl, N. Giladi, BR. Bloem. Freezing of Gait: A practical Approach to Management. Lancet Neurology, vol. 14, pp. 768-778, 2015.
[7] R. Iansek, M. Danoudis. Freezing of Gait in Parkinson's Disease: Its Pathophysiology and Pragmatic Approaches to Management. Movement Disorders: Clinical Practice pp. 290-297, 2016.
[8] M. Gilat, A.L.S. de-Lima, B.R. Bloem, J.M. Shine, J. Nonneks, S.J.G. Lewis. Freezing of Gait: Promising Avenues for Future Treatment. Parkinsonism and Related Disorders, vol. 52, pp. 7-16, 2018.
[9] M. Bachlin, M. Plotnik, D. Roggen, I. Maidan, J.M. Hausdorff, N. Giladi, and G. Troster. Wearable assistant for Parkinson's Disease patients with the Freezing of Gait symptom. IEEE Trans. on Information Technology in Biomedicine, vol. 14, no. 2, pp. 436-446, 2010.
[10] L. Palmerini, L. Rocchi, S. Mazilu, E. Gazit, J. M. Hausdorff, and L. Chiari. Identification of characteristic motor patterns preceding freezing of gait in Parkinsons disease using wearable sensors, Frontiers in neurology, vol. 8, p. 394, 2017.
[11] J. Camps, A. Samà, M. Martın, D. Rodrıguez-Martın, C. Perez-Lopez, J. M. M. Arostegui, J. Cabestany, A. Catala, S. Alcaine, B. Mestre et al., Deep learning for freezing of gait detection in Parkinson's disease patients in their homes using a waist-worn inertial measurement unit. Knowledge-Based Systems, vol. 139, pp. 119–131, 2018.
[12] S. Mazilu, A. Calatroni, E. Gazit, D. Roggen, J. M. Hausdorff, and G. Troster, Feature learning for detection and prediction of freezing of gait in Parkinson's disease, in International Workshop on Machine Learning and Data Mining in Pattern Recognition. pp. 144–158, Springer, 2013.
[13] D. De Venuto, V. F. Annese, G. Mezzina, and G. Defazio, FPGA-based embedded cyber-physical platform to assess gait and postural stability in Parkinson's disease, IEEE Transactions on Components, Packaging and Manufacturing Technology, Vol. 8, no. 7, 2018.
[14] B. T. Cole, S. H. Roy, and S. H. Nawab, Detecting freezing-of-gait during unscripted and unconstrained activity, in Annual International Conference of the IEEE Engineering in Medicine and Biology Society, pp. 5649–5652, 2011.
[15] J. C. Ayena, H. Zaibi, M. J.D. Otis, and B.A. J. Menelas, Home-based risk of falling assessment test using a closed-loop balance model, IEEE transactions on neural systems and rehabilitation engineering, vol. 24, no. 12, pp. 1351–1362, 2016.
[16] D. Sweeney, L.R. Quinlam, P. Browne, M. Richardson, P. Meskell, G. OLaighin. A Technological Review of Wearable Cueing Devices Addressing Freezing of Gait in Parkinson's Disease. Sensors, vol. 19, pp. 1277, 2019.
[17] P. A. Rochaa, G. M. Porfírio, H. B. Ferrazc, V. F. M. Trevisani. Effects of External Cues on Gait Parameters of Parkinson's Disease Patients: A Systematic Review. Clinical Neurology and Neurosurgery, vol. 124, pp. 127-134, 2014.
[18] S. Mazilu, M. Hardegger, Z. Zhu, D. Roggen, G. Troster, M. Plotnik, and J. M. Hausdorff, Online detection of freezing of gait with smartphones and machine learning techniques, in IEEE International Conference on Pervasive Computing Technologies for Healthcare., pp. 123–130, 2012.
[19] A. Samà, D. Rodrıguez-Martın, C. Perez-Lopez, A. Catala, S. Alcaine, B. Mestre, A. Prats, M. C. Crespo, and A. Bayes, Determining the optimal features in freezing of gait detection through a single waist accelerometer in home environments, Pattern Recognition Letters, 2017.
[20] D. Rodrıguez-Martın, A. Samà, C. Perez-Lopez, A. Catala, J. M. M. Arostegui, J. Cabestany, A. Bayes, S. Alcaine, B. Mestre, A. Prats et al., Home detection of freezing of gait using support vector machines through a single waist-worn triaxial accelerometer, PloS one, vol. 12, no. 2, 2017.
[21] K. Hu, Z. Wang, S. Mei, K. Ehgoetz, T. Yao, S. Lewis, and D. Feng, Vision-based freezing of gait detection with anatomic directed graph representation, IEEE Journal of Biomedical and Health Informatics, pp. 1–1, 2019.
[22] A. L. S. de Lima, L. J. Evers, T. Hahn, L. Bataille, J. L. Hamilton, M. A. Little, Y. Okuma, B. R. Bloem, and M. J. Faber, Freezing of gait and fall detection in Parkinson's disease using wearable sensors: a systematic review, J. of neurology, vol. 264, no. 8, pp. 1642–1654, 2017.
[23] R. Ramakrishnan, M. S. Ram, P. Pabitha, and R. S. Moorthy, Freezing of gait prediction in Parkinson's patients using neural network, in IEEE International Conference on Intelligent Computing and Control Systems, pp. 61–66, 2018.
[24] N. K. Orphanidou, A. Hussain, R. Keight, P. Lishoa, J. Hind, and H. Al-Askar, Predicting freezing of gait in Parkinson's disease patients using machine learning, in IEEE Congress on Evolutionary Computation, pp. 1–8, 2018.
[25] A. M. A. Handojoseno, J. M. Shine, T. N. Nguyen, Y. Tran, S. J. G. Lewis and H. T. Nguyen, The detection of Freezing of Gait in Parkinson's disease patients using EEG signals based on Wavelet decomposition, International Conference of the IEEE Engineering in Medicine and Biology Society, pp. 69-72, 2012.
[26] A. M. A. Handojoseno, J. M. Shine, T. N. Nguyen, Y. Tran, S. J. G. Lewis and H. T. Nguyen, Using EEG spatial correlation, cross frequency energy, and wavelet coefficients for the prediction of Freezing of Gait in Parkinson's Disease patients, International Conference of the IEEE Engineering in Medicine and Biology Society, pp. 4263-4266, 2013.
[27] N. Naghavi, A. Miller, E. Wade. Towards Real-Time Prediction of Freezing of Gait in Patients with Parkinson's Disease: Addressing the Class Imbalance Problem, Sensors, vol. 19, no. 18, 2019, pp. 3898.
[28] N. M. Nasrabadi, Pattern recognition and machine learning, Journal of electronic imaging, vol. 16, no. 4, 2007.
[29] R. A. Fisher, The use of multiple measurements in taxonomic problems, Annals of eugenics, vol. 7, no. 2, pp. 179–188, 1936.
[30] S. Mika, G. Ratsch, J. Weston, B. Scholkopf, and K.R. Mullers, Fisher discriminant analysis with kernels, in Neural networks for signal processing IX. IEEE signal processing society workshop, pp. 41–48, .
[31] D. M. Powers, Evaluation: from precision, recall and f-measure to roc, informedness, markedness and correlation, Journal of Machine Learning Technologies, vol. 2, no.1, pp.37—63, 2011.
[32] I. B. Mohamad and D. Usman, Standardization and its effects on k-means clustering algorithm, Research Journal of Applied Sciences, Engineering and Technology, vol. 6, no. 17, pp. 3299–3303, 2013.
[33] S. Seo, A review and comparison of methods for detecting outliers in univariate data sets, Ph.D. dissertation, University of Pittsburgh, 2006.
[34] F. Magrinelli, A. Picelli, P. Tocco, A. Federico, L. Roncari, N. Smania, G. Zanette, S. Tamburin. Pathophysiology of Motor Dysfuntion in Parkinson's Diseaseas the Rationale for Drug Treatment and Rehabilitation. Parkinson's Disease, no. 9832839, 2016.
[35] P. Redgrave, M. Rodriguez, Y. Smith, M.C. Rodriguez-Oroz, S. Lehericy, H. Bergman, Y.A. Mahlon, R. DeLong, J.A. Obeso. Goal-directed and habitual control in the basal ganglia: implications for Parkinson's disease. Nature Reviews: Neuroscience. Vol. 11, pp. 760-772, 2010.